A blind source separation based approach for modal parameter estimation in traditional input-output experimental modal analysis framework

Vikas Arora[1], Shashank Chauhan[2]

[1] Department of Technology and Innovation, University of Southern Denmark, Campusvej 55, Odense 5230, Denmark viar@iti.sdu.dk

[2] Brüel & Kjær Sound & Vibration Measurement A/S Skodsborgvej 307 DK-2850 Nærum, Denmark schauhan@bksv.com

ABSTRACT

Though Blind Source Separation (BSS) techniques have typically been applied within Operational Modal Analysis (OMA) framework, there joint diagonalization property can also be utilized within traditional input-output Experimental Modal Analysis (EMA) for the purpose of modal parameter estimation. This paper explores this possibility and suggests an approach to achieve the same. The paper presents the mathematical concepts that make it possible for Second Order Blind Identification (SOBI), a blind source separation algorithm to be applied to impulse response functions for the purpose of modal parameter estimation. It is also shown in the paper that, in its current form, the approach provides real mode shapes, irrespective of the nature of the system under investigation. In addition to demonstrating the approach by means of studies conducted on an analytical 5 degrees-of-freedom system, the real mode shapes extracted using the suggested approach are also used for model updating purposes.

Keywords: Blind Source Separation, modal parameter estimation, Second Order Blind Identification, joint-diagonalization, model updating

1. Introduction

Blind Source separation (BSS) [1, 2] techniques aim at solving the problem of mixed source signals. Goal is to identify the source signals, and the mixing matrix, solely on the basis of observed mixed signals. The procedure applied to achieve this goal often involves exploitation of higher order statistics, as many techniques use mutual independence [1] as the guiding principle for source separation. However, there are several applications where second order statistics suffice. Application of BSS in the field of modal analysis is one such example.

In last few years, there has been tremendous interest in utilizing BSS techniques for modal analysis purposes [3-7]. Most of these works are oriented towards application of BSS techniques to Operational Modal Analysis (OMA). In OMA, one aims at identifying the modal parameters of a dynamic system based on only measured output responses. This is in contrast to traditional modal analysis, where knowledge of input force excitation is also available, and utilized, for modal parameter estimation. OMA lines up well with BSS and both are seemingly analogous. However, mathematically BSS can be looked upon as a decomposition, whose central idea is joint diagonalization. Thus, there is no reason why it cannot be applied to cases that are not 'blind' per se.

This paper develops this idea and explores the possibility of applying BSS to traditional modal analysis. The paper utilizes a second order BSS technique, *Second Order Blind Identification* (SOBI) for this purpose. This technique is described in section 2.1. The mathematical basis of application of SOBI to traditional modal analysis is presented in section 2.2. It is shown in this section how joint diagonalization of measured impulse response functions can be utilized for estimating modal parameters.

One of the salient features of the procedure explained in this paper is that irrespective of the actual system characteristics, suggested method always estimates real mode shapes. This apparent limitation of the proposed method, can however be exploited effectively by noting that one typically needs real mode shapes for finite element model updating purposes. Thus, even though the true mode shape is complex in nature, for model updating purposes it is first normalized such that it becomes real. This paper looks into these possibilities as well, beginning with section 3 where a recap of natural frequency and mode shape based model-updating procedure is provided.

The ideas put forth in this paper are validated by means of studies conducted on a numerical 5 degrees-of-freedom (DOF) system, as presented in section 4. The properties of this system are changed to investigate variety of cases and evaluate the performance of proposed technique. The section ends with the results of model updating procedure for two separate cases in which different stiffness values of the lumped mass system are updated.

2. BSS and Modal Analysis

Most Blind Source Separation (BSS) based Operational Modal Analysis (OMA) techniques have modal expansion theorem [8] as their foundation. Modal expansion theorem states that response of a structure can be expressed as a linear combination of the modal vectors. Mathematically, this is represented as

$$\mathbf{x}(\mathrm{t}) = \mathbf{\Phi}\,\boldsymbol{\eta}(\mathrm{t}) \tag{1}$$

where, $\mathbf{x}(\mathrm{t})$ is the response of the structure, $\mathbf{\Phi}$ is matrix of modal vectors and $\boldsymbol{\eta}(\mathrm{t})$ are modal coordinates or principal coordinates. This mathematical relationship also forms the basis of modal coordinate transformation, which uncouples the equations of motion of a multiple degrees-of-freedom system into several simpler single degrees-of-freedom equations.

As has been noted in several works [1, 2], BSS algorithms aim at finding the original source signals and the corresponding mixing matrix that generated the output response signals. The mathematical relation that BSS algorithms exploit is similar to Eq. 1 and is given as

$$\mathbf{x}(\mathrm{t}) = \mathbf{A}\,\mathbf{s}(\mathrm{t}) \tag{2}$$

Under certain conditions, such as when source signals have a temporal structure with different autocorrelation functions and are mutually uncorrelated, it is possible to extract the source signals **s**(t) and the mixing matrix **A**, which is assumed to be real. In general, BSS techniques require source signals to be statistically mutually independent (not just mutually uncorrelated). This is what enables higher order statistics based BSS algorithms to operate on response signals, **x**(t). However, from the point of view of OMA, it suffices that they are mutually uncorrelated as this is the case with modal coordinates (which are analogous to source signals in Eq. 2). Thus, most BSS based OMA algorithms are based on second order statistics.

2.1 Second Order Blind Identification (SOBI) Algorithm

Second Order Blind Identification (SOBI) [9] is a BSS algorithm that lends itself very well to the cause of modal parameter estimation task in OMA. This algorithm jointly diagonalizes the output response covariance matrices at various time lags in order to obtain modal vectors $\mathbf{\Phi}$ and modal coordinates $\boldsymbol{\eta}(\mathrm{t})$, which provide the estimate of the modal frequency and damping. SOBI algorithm is briefly explained below,

1. Estimate the covariance matrix of the output observations *x*

$$\hat{R}_x(0) = \frac{1}{N}\sum_{k=1}^{N} x(k)x^T(k) \tag{3}$$

where $\hat{R}_x(0)$ is the covariance matrix at zero time lag and N is the total number of time samples taken.

2. Compute EVD (or SVD) of $\hat{R}_x(0)$

$$\hat{R}_x(0) = V_x\Lambda_x V_x^T = V_s\Lambda_s V_s^T + V_N\Lambda_N V_N^T \tag{4}$$

where V_s is m X n matrix of eigenvectors associated with n principal eigenvalues of $\Lambda_s = diag\,(\lambda_1, \lambda_2, ..., \lambda_n)$ in descending order. V_n is m X (m-n) matrix containing the (m-n) noise eigenvectors associated with noise eigenvalues $\Lambda_n = diag\,(\lambda_{n+1}, \lambda_{n+2}, ..., \lambda_m)$. The number of sources n are thus estimated based on the n most significant eigenvalues (or singular values in case of SVD).

3. Perform pre-whitening transformation

$$\bar{x}(k) = \Lambda_s^{-1/2} V_s^T x(k) = Qx(k) \qquad 5)$$

4. Estimate the covariance matrix of the vector $\bar{x}(k)$ for preselected time lags other than p=0. Perform SVD on the estimated covariance matrix.

$$\hat{R}_{\bar{x}}(p) = \frac{1}{N} \sum_{k=1}^{N} \bar{x}(k) \;\; \bar{x}^T(k-p) = U_{\bar{x}} \Sigma_{\bar{x}} V_{\bar{x}}^T \qquad 6)$$

5. Perform Joint Approximate Diagonalization on the above set of covariance matrices to estimate the orthogonal matrix U that diagonalizes a set of covariance matrices.

$$\hat{R}_{\bar{x}}(p_i) = U_{\bar{x}} \Sigma_{\bar{x}}(p_i) U_{\bar{x}}^T \qquad 7)$$

6. The mixing matrix and source signals can be estimated as

$$\hat{A} = Q^+ U_{\bar{x}} = V_s \Lambda_s^{1/2} U_{\bar{x}} \qquad 8)$$

$$y(k) = \hat{s}(k) = U_{\bar{x}}^T \bar{x}(k) \qquad 9)$$

2.2 Extension of SOBI to Experimental Modal Analysis

The joint diagonalization procedure employed by SOBI, as explained above, can also be employed within the framework of traditional experimental modal analysis, where one also measures the excitation forces in addition to the output responses. In this section, SOBI is extended to traditional modal analysis.

The impulse response function, for a MDOF system, at a particular output degree of freedom (dof) *p*, due to excitation force applied at dof *q*, is expressed in terms of modal parameters, i.e. modal frequency λ_r and residue A_{pqr} as

$$h_{pq}(t) = \sum_{r=1}^{N} A_{pqr}\, e^{\lambda_r t} + A_{pqr}^*\, e^{\lambda_r^* t} \qquad 10)$$

This can be further written in the following manner [10] (residue $A_{pqr} = \frac{R_{pqr}}{2j}$),

$$h_{pq}(t) = \sum_{r=1}^{N} R_{pqr}\, e^{\sigma_r t} \sin(\omega_r t) \qquad 11)$$

where ω_r is the damped natural frequency of the system and σ_r is the associated damping. For the undamped/proportionally damped case, the above equation reduces to the same form as Eq. 1. This is also analogous to the modal expansion theorem expressed in Eq. 2. It is worth noting at this point that the modal expansion theorem is only applicable for undamped or proportionally damped systems. This similarity between Eq. 1 (and Eq. 2) and Eq. 11 presents a possibility of applying SOBI to impulse response functions and obtain corresponding modal parameters, as long as the assumption regarding the damping are true.

For the single input multiple output (SIMO) case, the impulse response functions can be mathematically expressed as

$$\mathbf{h}(t) = \mathbf{R}\,\overline{\boldsymbol{\eta}}(t) \qquad 12)$$

where $\mathbf{h}(t)$ is a vector of impulse response functions at various output dofs due to force applied at a specific input dof. $\mathbf{R}$ is then a matrix of residues, whose columns can be expressed in terms of modal vector $\boldsymbol{\varphi}_r$ and participation vector. For SIMO case, participation vector is essentially a scalar given as $L_{ir} = q_r \phi_{ir}$, where q_r is the scaling factor associated with the r^{th} mode and ϕ_{ir} is the modal coefficient associated with that mode at the input excitation dof *i*. The mode shape information can thus be extracted from the residue vector estimated using SOBI. Frequency and damping information can be estimated from $\overline{\boldsymbol{\eta}}(t)$ using simple SDOF methods.

3. Utilizing BSS mode shapes for model updating

Eqs. 1 and 11 are key to utilizing SO-BSS algorithms for modal analysis purposes. They are analogous to the BSS mixing model shown in Eq. 2. However, the issue with this model is that it assumes the mixing matrix to be real. In terms of modal analysis, it means that the dynamic system under investigation is assumed to be undamped or proportionally damped, meaning that the modes are real normal. However, in real world, dynamic structures do not always adhere to these assumptions. Real world structures often exhibit dynamic characteristics with complex modes. This is one major limitation of the approach suggested in section 2.2. However, this limitation can turn out to be an advantage in case of model updating. Model updating techniques often require experimentally estimated mode shapes (often complex) to be first normalized such that they are real. It is these normalized real mode shapes that are utilized for model updating purposes. Since the procedure suggested in section 2.2 provides real mode shapes directly, one can immediately use them for model updating. In this context, it is apt to recall model updating theory.

It is well known that finite element predictions are often called into question when they are in conflict with test results [11]. Inaccuracies in finite element model, and errors in results predicted by them, can arise due to use of incorrect modeling of boundary conditions, incorrect modeling of joints, and difficulties in modeling of damping etc. This has led to the development of model updating techniques, which aim at reducing the inaccuracies present in finite element model in the light of measured dynamic test data. A number of model updating methods have been proposed in recent years, as shown in the surveys [12, 13], most of which use modal data, i.e. natural frequencies and mode shapes for the purpose of updating the finite element model.

Collins et al. [14] use the natural frequency and modeshape sensitivity for finite element model updating in an iterative framework. The updating parameters (p_i), corresponding to finite element model, are corrected to bring the analytical modal data closer to that obtained experimentally. For the r[th] eigenvalue, λ^r (square of the r[th] natural frequency in rad/sec), and the r[th] eigenvector, $\{\Phi\}^r$ (the mode shape), linearization gives:

$$\lambda_X^r = \lambda_{FE}^r + \sum_{i=1}^{nu}\left(\frac{\partial \lambda_{FE}^r}{\partial p_i}\cdot \Delta p_i\right) \qquad 13)$$

$$\{\Phi\}_X^r = \{\Phi\}_{FE}^r + \sum_{i=1}^{nu}\left(\frac{\partial \{\Phi\}_{FE}^r}{\partial p_i}\cdot \Delta p_i\right) \qquad 14)$$

where subscript FE and X denote finite element model and experimental model respectively. *nu* represents number of updating parameters. The derivative of eigenvalues and mode shapes can be calculated from the following relationship given by Fox and Kapoor [15],

$$\frac{\partial \lambda_{FE}^r}{\partial p_i} = \frac{\{\phi\}_{FE}^{rT}\left[\frac{\partial [K]}{\partial p_i} - \lambda_{FE}^r \frac{\partial [M]}{\partial p_i}\right]\{\phi\}_{FE}^r}{\{\phi\}_{FE}^{rT}[M]\{\phi\}_{FE}^r} \qquad 15)$$

$$\frac{\partial\{\Phi\}_{FE}^{r}}{\partial p_i}=\sum_{j=1,\neq r}^{N}\left(\frac{\{\phi\}_{FE}^{jT}\left[\frac{\partial[K]}{\partial p_i}-\lambda_{FE}^{r}\frac{\partial[M]}{\partial p_i}\right]\{\phi\}_{FE}^{j}}{\left(\lambda^{r}-\lambda^{j}\right)}\right)-\frac{1}{2}\{\phi\}_{FE}^{rT}\frac{\partial[M]}{\partial p_i}\{\phi\}_{FE}^{r} \qquad 16)$$

Using the above equations, the finite element model updating for resonance frequencies and modeshapes can be written for m number of modes as:

$$\begin{Bmatrix}\lambda_X^1-\lambda_{FE}^1/\lambda_{FE}^1\\ \{\Phi\}_X^1-\{\Phi\}_{FE}^1\\ \vdots\\ \vdots\\ \vdots\\ \lambda_X^m-\lambda_{FE}^m/\lambda_{FE}^m\\ \{\Phi\}_X^m-\{\Phi\}_{FE}^m\end{Bmatrix}=\begin{bmatrix}\frac{\partial\lambda_{FE}^1}{\partial p_1}\Big/\lambda_{FE}^1 & \frac{\partial\lambda_{FE}^1}{\partial p_2}\Big/\lambda_{FE}^1 & \cdots\ \cdots\ \cdots & \frac{\partial\lambda_{FE}^1}{\partial p_{nu}}\Big/\lambda_{FE}^1\\ \frac{\partial\{\Phi\}_{FE}^1}{\partial p_1} & \frac{\partial\{\Phi\}_{FE}^1}{\partial p_2} & \cdots\ \cdots\ \cdots & \frac{\partial\{\Phi\}_{FE}^1}{\partial p_{nu}}\\ \cdots & \cdots & \cdots\ \cdots\ \cdots & \cdots\\ \cdots & \cdots & \cdots\ \cdots\ \cdots & \cdots\\ \cdots & \cdots & \cdots\ \cdots\ \cdots & \cdots\\ \frac{\partial\lambda_{FE}^m}{\partial p_1}\Big/\lambda_{FE}^m & \frac{\partial\lambda_{FE}^m}{\partial p_2}\Big/\lambda_{FE}^m & \cdots\ \cdots\ \cdots & \frac{\partial\lambda_{FE}^m}{\partial p_{nu}}\Big/\lambda_{FE}^m\\ \frac{\partial\{\Phi\}_{FE}^m}{\partial p_1} & \frac{\partial\{\Phi\}_{FE}^m}{\partial p_2} & \cdots\ \cdots\ \cdots & \frac{\partial\{\Phi\}_{FE}^m}{\partial p_{nu}}\end{bmatrix}\cdot\begin{Bmatrix}\Delta p_1\\ \Delta p_2\\ \vdots\\ \vdots\\ \vdots\\ \Delta p_{nu}\end{Bmatrix} \qquad 17)$$

where $\{\Delta p\}$ is a vector of change in updating parameters. It can be observed from Eq. 17 that values of updating parameters are mostly affected by eigenvalues as magnitude of eigenvalues is significantly higher than eigenvectors. In order to include the effect of changes in eigenvectors, the ratio of eigenvalues is considered in this problem formulation.

4. Investigations on an Analytical 5 DOF system

4.1 Modal Parameter Identification

A simple 5 DOF system as shown in Fig. 1 is selected to investigate the applicability of the proposed method. The associated mass and stiffness matrix for this system are listed below.

$$\mathbf{M}=\begin{bmatrix}250&0&0&0&0\\0&350&0&0&0\\0&0&30&0&0\\0&0&0&450&0\\0&0&0&0&50\end{bmatrix} \qquad \mathbf{K}=1000\times\begin{bmatrix}9000&-5000&0&0&0\\-5000&11000&-6000&0&0\\0&-6000&12500&-6500&0\\0&0&-6500&14500&-8000\\0&0&0&0&15000\end{bmatrix}$$

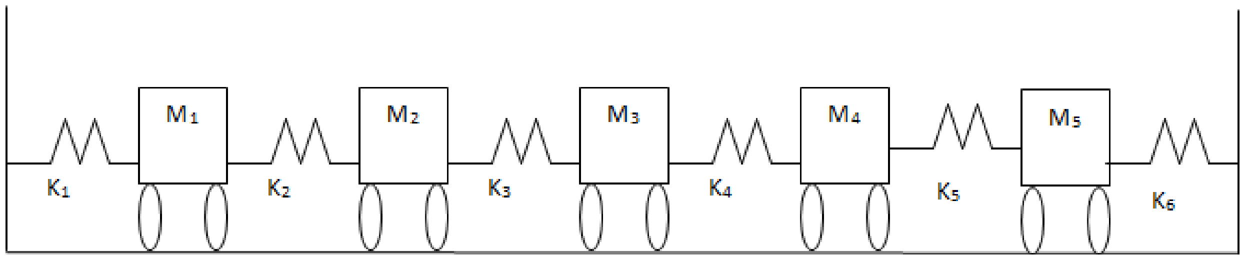

Figure 1: 5 DOF Lumped Mass system

4.1.1 Case 1 - Undamped System

To begin with, the above-mentioned system is considered undamped. Since the current version of proposed approach is formulated for SIMO scenario, the third column of the impulse response matrix, $\mathbf{h}_{:,3}$ is considered in this study. It should be noted that the algorithm was set up to jointly diagonalize the first 1500 time lags of IRFs. A comparison of estimated natural frequencies with theoretical values is provided in Table 5 at the end of this section. This table lists and compares the natural frequencies from various cases investigated in this study. Mode shape comparison is given in Table 1.

Table 1: Modal Shape Comparison for undamped system

DOF	Mode 1		Mode 2		Mode 3		Mode 4		Mode 5	
	Theo.	Est.	Theo.	Est.	Theo.	Est.	Theo.	Est.	Theo.	Est.
1	1	1	1	1	1	1	1	1	1	1
2	1.4904	1.4904	0.8376	0.8377	-0.6026	-0.6025	-13.669	-13.712	-19.872	-19.872
3	1.3608	1.3611	-0.2382	-0.2397	-0.2490	-0.2500	220.79	222.254	465.19	465.19
4	1.2022	1.2022	-1.2100	-1.2099	0.1326	0.1327	121.92	121.44	-17.687	-17.687
5	0.6547	0.6547	-0.6896	-0.6896	0.0842	0.0842	-2080.6	-2073.2	21.206	21.206

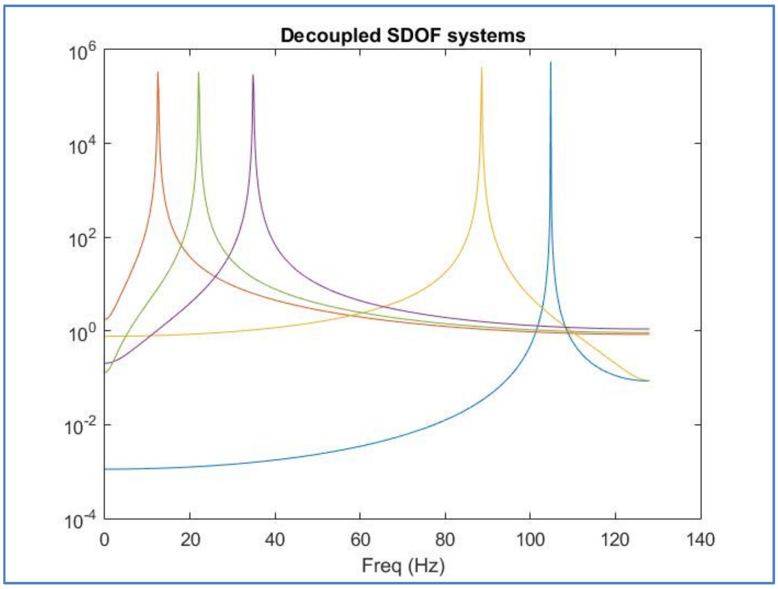

Figure 2: Power spectra of decoupled modes (Undamped System)

The separation using SOBI, illustrated in Fig. 2, shows the power spectra of decoupled SDOF systems, calculated on the basis of estimated $\overline{\boldsymbol{\eta}}(t)$. It is noticeable that estimated mode shapes match very well with theoretical values. The only error noticeable, although very small, is for the fourth mode.

4.1.2 Case 2 – Light Proportional Damping

Next, damping is introduced to the above-mentioned 5 DOF system and several possibilities are considered. To begin with damping is considered as proportional, $\mathbf{C} = 1.3\mathbf{M} + 4e^{-6}\mathbf{K}$. Modal vectors in this case are still real and same as that listed in Table 2 along with estimated mode shapes. Note that modal frequency and damping for this proportionally damped case are listed in Table 5 and 6. The power spectra of estimated SDOF systems (Fig. 3) again shows that the system modes are decoupled satisfactorily by SOBI. The mode shape estimates compare well in this case also.

Table 2: Modal Matrix (Light proportional damping)

DOF	Mode 1		Mode 2		Mode 3		Mode 4		Mode 5	
	Theo.	Est.	Theo.	Est.	Theo.	Est.	Theo.	Est.	Theo.	Est.
1	1	1	1	1	1	1	1	1	1	1
2	1.4904	1.4906	0.8376	0.8366	-0.6026	-0.6024	-13.669	-18.247	-19.872	-19.968
3	1.3608	1.3608	-0.2382	-0.2361	-0.2490	-0.2461	220.79	279.94	465.19	467.28
4	1.2022	1.2024	-1.2100	-1.2107	0.1326	0.1326	121.92	162.58	-17.687	-17.772
5	0.6547	0.6548	-0.6896	-0.6898	0.0842	0.0843	-2080.6	-2774.8	21.206	21.298

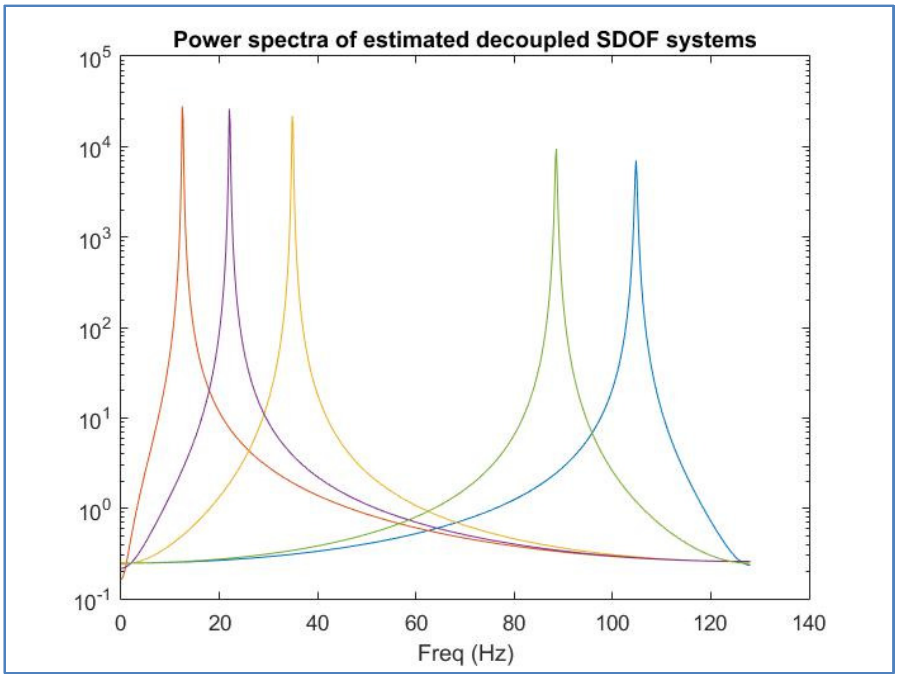

Figure 3: Power spectra of decoupled modes (Light Proportional Damping)

4.1.3 Case 3 – Moderate Proportional Damping

In this case, damping is still considered to be proportional but it is adjusted so that the values are moderate. This is achieved by using the following value, $\mathbf{C} = 1.3\mathbf{M} + 9e^{-5}\mathbf{K}$. The theoretical and estimated mode shapes are listed in Table 3. The power spectra of separated modes, shown in Fig. 4, indicates that separation is not as complete as is the case with previous scenarios.

This can be seen in the power spectra of 5th mode. The comparison of estimated frequency and damping is provided in Table 5 and 6.

Table 3: Modal Matrix (Moderate proportional damping)

DOF	Mode 1		Mode 2		Mode 3		Mode 4		Mode 5	
	Theo.	**Est.**	**Theo.**	**Est.**	**Theo.**	**Est.**	**Theo.**	**Est.**	**Theo.**	**Est.**
1	1	1	1	1	1	1	1	1	1	1
2	1.4904	1.4907	0.8376	0.8320	-0.6026	-0.6008	-13.669	61.766	-19.872	-21.876
3	1.3608	1.3612	-0.2382	-0.2387	-0.2490	-0.2435	220.79	-1234.0	465.19	510.14
4	1.2022	1.2027	-1.2100	-1.2115	0.1326	0.1325	121.92	-71.371	-17.687	-19.351
5	0.6547	0.6549	-0.6896	-0.6900	0.0842	0.0847	-2080.6	1918.9	21.206	21.278

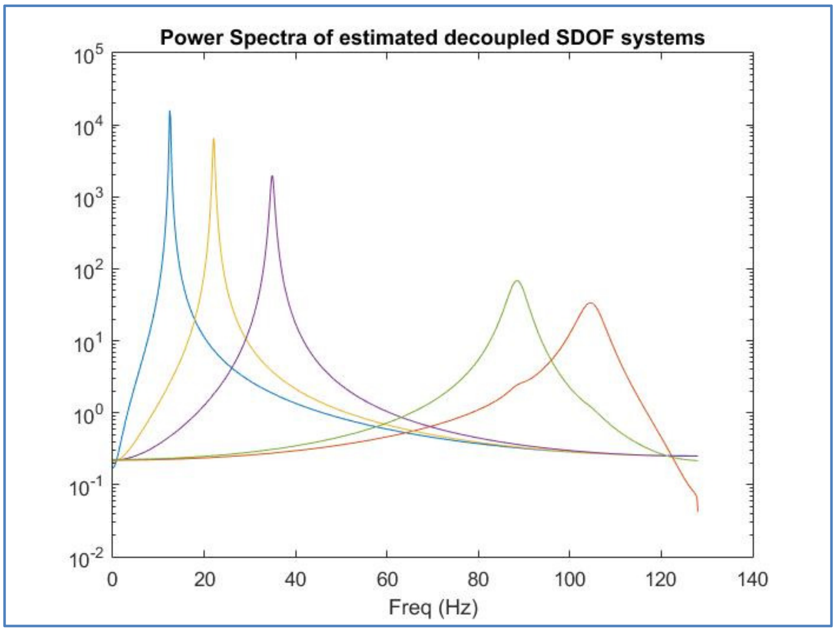

Figure 4: Power spectra of decoupled modes (Moderate Proportional Damping)

4.1.4 Case 4 – Non-proportional Damping

Previously, damping is either neglected or considered proportional. Here, the effects of non-proportional damping are studied. The chosen damping matrix is given as

$$\mathbf{C}=\begin{bmatrix} 3250 & -250 & 0 & 0 & 0 \\ -250 & 450 & -200 & 0 & 0 \\ 0 & -200 & 320 & -120 & 0 \\ 0 & 0 & -120 & 190 & -70 \\ 0 & 0 & 0 & -70 & 270 \end{bmatrix}$$

Theoretical modal parameters (frequency and damping) for the non-proportionally damped case are listed in Table 5 and 6. Modal vectors in this case become complex and are listed in Table 4 along with estimated vectors, which are expectedly real. The power spectra plots (Fig. 5) for this case clearly show that decoupling of impulse response functions into simple SDOF system responses is not as accurate. This is expected as the method is formulated on the assumption that the system is either undamped or proportionally damped, which is not the case here.

Table 4: Estimated Modal Vectors (Non-proportional damping)

Mode 1		Mode 2		Mode 3		Mode 4		Mode 5	
Theo.	**Est.**	**Theo.**	**Est.**	**Theo.**	**Est.**	**Theo.**	**Est.**	**Theo.**	**Est.**
1.0000 + 0.0000i	1	1.0000 + 0.0000i	1	1.0000 + 0.0000i	1	1.0000 + 0.0000i	1	1.0000 + 0.0000i	1
1.4899 + 0.0382i	1.4921	0.8371 + 0.0640i	0.8167	-0.6008 + 0.0447i	-0.5942	-13.6554 + 0.5907i	14.5782	-19.8548 + 0.7166i	-21.1548
1.3601 + 0.0457i	1.3628	-0.2377 + 0.0296i	-0.2441	-0.2487 + 0.0127i	-0.2459	220.4414 - 11.8562i	-201.537	464.6472 - 19.5550i	493.378
1.2014 + 0.0505i	1.2045	-1.2086 - 0.0065i	-1.2486	0.1317 - 0.0164i	0.1111	121.8771 - 4.4640i	-112.067	-17.6589 + 0.8717i	-18.7556
0.6543 + 0.0273i	0.6559	-0.6888 - 0.0037i	-0.7105	0.0836 - 0.0099i	0.0732	-2079.5864 + 68.45084i	1917.989	21.1400 - 1.5169i	22.4043

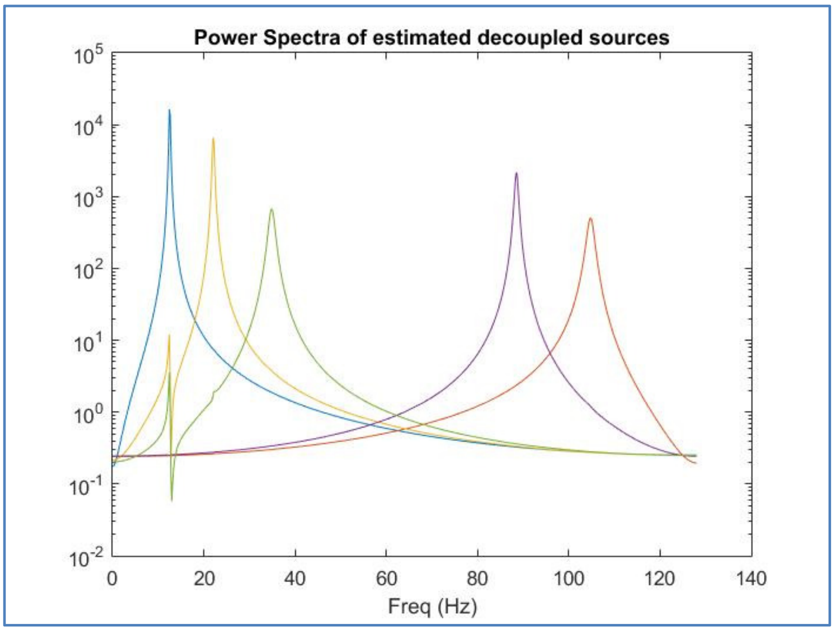

Figure 5: Power spectra of decoupled modes (Non-proportional Damping)

4.2 Modal frequency and damping comparison

Table 5 and 6 provide the comparison of theoretical and estimated frequency and damping values for the four cases studied in last section. Results show that the estimated values compare well with theoretical parameters.

Table 5: Comparison of modal frequencies

Undamped		Light Proportional Damping		Moderate Proportional Damping		Non-proportional Damping	
Theo. (Hz)	Est. (Hz)	Theo. (Hz)	Est. (Hz)	Theo. (Hz)	Est. (Hz)	Theo. (Hz)	Est. (Hz)
12.5234	12.5672	12.5230	12.5295	12.5226	12.5336	12.5263	12.5317
22.0805	22.1070	22.0803	22.0828	22.0792	22.0900	22.0830	22.0923
34.8880	34.9054	34.8878	34.8904	34.8851	34.8931	34.8635	34.8782
88.5248	88.5651	88.5246	88.5230	88.4944	88.4275	88.5238	88.5210
104.7825	104.8246	104.7822	104.7735	104.7334	104.3835	104.7787	104.7354

Table 6: Comparison of modal damping

Light Proportional Damping		Moderate Proportional Damping		Non-proportional Damping	
Theo. (%)	Est. (%)	Theo. (%)	Est. (%)	Theo. (%)	Est. (%)
0.8418	0.8303	1.1801	1.1874	1.1486	1.1411
0.4963	0.4928	1.0928	1.0971	1.0589	1.0643
0.3404	0.3413	1.2830	1.2809	2.1720	2.1653
0.2281	0.2278	2.6198	2.6226	0.4872	0.4876
0.2304	0.2306	3.0614	3.0748	0.8423	0.8329

4.3 Investigations related to model updating

Choice of updating parameters on the basis of engineering judgment about the possible locations of modeling errors in a structure is one of the strategies to ensure that only physically meaningful corrections are made. While using the mode shapes estimated using SOBI in previous section, for model updating purposes, two different cases are considered. First, stiffness K_1 is considered as an updated parameter and later stiffness K_3. In case of 5 degrees-of-freedom lumped mass system, modeling of stiffness at the ends is expected to be a dominant source of inaccuracy in the FE model assuming that the values of material and the geometric parameters are correctly known. The modeshape and natural frequencies extracted for 4 different cases have been used to update the stiffness K_1. The updated values of the stiffness K_1 and corresponding errors are provided in the Table 7. It can be observed from the Table 7 that, after updating, the error in all the cases have been less than 2%, which is acceptable.

Table 7: Stiffness values of spring K_1 after updating

Cases	Updated values	% Error
Undamped system	4.0603×10^6	-1.5079
Lightly proportional damped	4.0303×10^6	-0.7582
Moderate proportional damped	4.0718×10^6	-1.7951
Non-proportional damping	4.0615×10^6	-1.5384

Next K_3 has been considered as updated parameter. The reason for choosing K_3 is that SOBI is applied to the SIMO case where the structure is excited at location 3. It can be observed from the updated values of K_3, given in Table 8 that after updating the error is very small.

Table 8: Stiffness values of spring K_3 after updating

Cases	Updated values	% Error
Undamped system	6.0226 X10^6	-0.3773
Lightly proportional damped	5.8769 X10^6	2.0510
Moderate proportional damped	5.8988 X10^6	1.6869
Non-proportional damping	5.9900 X10^6	1.5384

4.3 Discussions

Results listed in previous section show that proposed approach of applying SOBI to impulse response functions for modal parameter estimation purposes yields satisfactory results. The frequency and damping estimates compare well in most cases and the same can be said for mode shapes in general.

It is a feature of the proposed approach that mode shape matrix is estimated directly in the first step itself (mode shape matrix is analogous to mixing matrix). Expectedly, estimated mode shapes are real, irrespective of the nature of the dynamic system under investigation. There is no direct way of comparing them with theoretical mode shapes (which can be complex in certain cases). For cases such as undamped and proportionally damped system, modal coefficients compare well. It should be noted that applied algorithm is a SIMO algorithm and the chosen input DOF might not be able to excite all the modes equally. In all cases however, the modal assurance criteria (MAC) is close to 1. The biggest error in mode shapes is observed for moderately damped proportional damping case, where the mode shape associated with the fourth mode (third modal coefficient in particular) is not estimated with high accuracy. It is worth investigating if this can be improved by choosing a different excitation point. The performance with regards to non-proportional damping case is however satisfactory.

The results from finite element updating procedure show the effectiveness of this approach as the real mode shapes can be directly utilized for model updating procedure. The reported errors on the updated parameter is relatively low. However, the true measure of the advantage of this approach, for the purpose of model updating, can only be assessed by evaluating its performance vis-à-vis conventional techniques, which provide complex mode shape that are required to be normalized to obtain real mode shapes. The error on updating parameter using these two different approaches can provide more insight into the effectiveness of BSS based approach.

5. Conclusions

BSS algorithms have typically been employed in modal analysis domain within OMA framework. This is obvious as, like BSS, aim of OMA is to obtain modal parameters only on the basis of measured output responses. This paper treats BSS as a second order mathematical decomposition and exploits the joint diagonalization properties of SOBI to derive a new approach that is applicable to traditional experimental modal analysis framework where both input and output are known. The applicability and effectiveness of this approach is shown in this paper by means of investigations done on a numerical lumped mass system. The obtained results are satisfactory.

The suggested approach has a property that it provides real mode shapes irrespective of the nature of the dynamic system being analyzed. This is a drawback of the suggested approach but this property can be exploited for model updating purposes. The feasibility study carried out in this paper shows promise in terms of utilizing mode shapes obtained from this approach. However, as noted earlier, a complete picture can only emerge after comparing this approach with conventional approaches, where estimated mode shapes are normalized to get real mode shapes.

References

1. Cichocki, A., Amari, S., *Adaptive blind signal and image processing*. John Wiley and Sons, New York, 2002.
2. Hyvarinen, A., Karhunen, J., Oja, E., *Independent Component Analysis*. John Wiley and Sons, New York, 2001.
3. Antoni, J., "Blind separation of vibration components: principles and demonstrations", Mechanical Systems and Signal Processing 19 (6) (2005) 1166-1180.
4. Poncelet, F., Kerschen, G., Golinval, J.C., Verhelst, D., "Output-only modal analysis using blind source separation techniques", Mechanical systems and signal processing 21(6) (2007) 2335-2358.
5. Chauhan, S., Martell, R., Allemang, R.J., Brown, D.L., "Application of independent component analysis and blind source separation techniques to operational modal analysis", Proceedings of the 25th IMAC, Orlando (FL), USA, 2007.
6. Swaminathan, B., Sharma, B., Chauhan, S., "Utilization of blind source separation techniques for modal analysis", Proceedings of the 28th IMAC, Jacksonville (FL), USA, 2010.
7. Antoni, J., Chauhan, S., "A study and extension of second-order blind source separation to operational modal analysis," Journal of Sound and Vibration, vol. 332, no. 4, pp. 1079– 1106, Feb. 2013.
8. Allemang, R.J., *Vibrations: Experimental modal analysis.* UC-SDRL-CN-20-263-663/664, Structural Dynamics Research Laboratory, Department of Mechanical, Industrial and Nuclear Engineering, University of Cincinnati, 1999.
9. Belouchrani, A., Abed-Meraim, K.K., Cardoso, J.F., Moulines, E., "Second order blind separation of correlated sources", Proceedings of International Conference on Digital Signal Processing, pp. 346-351, 1993.
10. Allemang, R.J., *Vibrations: Analytical and Experimental modal analysis*. UC-SDRL-CN-20-263-662, Structural Dynamics Research Laboratory, Department of Mechanical, Industrial and Nuclear Engineering, University of Cincinnati, 1999.
11. Ewins D.J., *Modal testing: Theory, Practice and Application*. Research Studies Press England, 2000.
12. Friswell, M.I., Mottershead, J.E., *Finite element model updating in structural dynamics*. Kluwer Academic Publishers, Dordrecht, Netherlands, 1995.
13. Imregun, M., Visser W.J., "A review of model updating techniques", Shock and Vibration Digest, 23, 141-162, 1991.
14. Collins J.D., Hart G.C., Hasselman T.K., Kennedy B., "Statistical identification of structures", AIAA Journal, 12, 185-190, 1974.
15. Fox, R.L., Kapoor, M.P., "Rate of change of eigenvalues and eigenvectors", AIAA Journal, 12, 2426-2429, 1968.